Quantifying the commutation error of a BLDC machine using sensorless load angle estimation

Jasper De Viaene[1], Florian Verbelen[1], Michiel Haemers[1], Stijn Derammelaere[1], Kurt Stockman[1]
[1]Department of Industrial System and Product Design, Ghent University Campus Kortrijk, Belgium
E-mail: Jasper.DeViaene@UGent.be

***Abstract* —BLDC motors are often used for high speed applications, for example in pumps, ventilators and refrigerators. For commutation discrete position information is necessary. This feedback is often provided by Hall sensors instead of more expensive encoders. However, even small misalignment of the Hall sensors in low cost BLDC motors can lead to unwanted torque ripples or reduced performance of BLDC motors. This misplacement leads not only to noise and vibrations caused by the torque ripples but also to lower efficiency. In this paper, a self-sensing technique to assess the misalignment is introduced. The objective is to obtain knowledge of the quality of the commutation by quantifying the misalignment. The method used in this paper is based on the fundamental components of voltage and current measurements and only needs the available current and voltage signals and electrical parameters such as resistance and inductance to estimate the misalignment.**

***Index Terms*—Brushless DC motor, commutation, Hall sensors, load angle estimation, SDFT**

I. Introduction

BLDC motors are often used in applications with pumps, ventilators and refrigerators [1]–[3]. In this high speed applications is energy efficiency an important aspect. By the absence of the mechanical commutator, high speed and torque levels can be reached, wear of brushes and electrical sparks are avoided [4]. Because the commutation is done electronically, knowledge about the position is required. Inaccurate position information can lead to commutation errors. Optimizing the commutation is preferable to minimize torque ripples and obtain optimal performance [5], [6]. In this paper, a method is proposed to estimate the load angle of a 3-phase BLDC motor. The algorithm, based on a SDFT, estimates the fundamental components of electrical measurements and determine the position of the back emf in order to obtain information about the load angle [7], [8]. The load angle is an indication for the quality of the commutation.

II. Construction and Operation

A BLDC motor is a permanent magnet synchronous motor with trapezoidal back EMF. The motor consists of a permanent magnet rotor and a stator, which contains the three-phase star connected windings. The magnets are mounted on the surface of the magnetic material of the rotor [9]. This specific construction of the rotor and stator, results in a trapezoidal back EMF as depicted in blue in Fig. 1, [10]. For optimal torque generation, square waves, aligned with the back EMF, are the most commonly used current setpoints to drive a BLDC motor at optimal performance [11]. To become the alignment of the back emf and current setpoints, discrete position information has to be known. Information about these right commutation moments are usually derived from Hall sensors or sensorless algorithms detecting the zero crossings of the back EMF's [12]. Because the shape of the back EMF is position depending and is not known or directly measurable, the Hall sensors indicate when the back EMF in the phases changes. The positioning of the Hall sensors with respect to the concentrated windings define the quality of aligning of the rectangular stator currents and the back EMF, which is essential to minimize torque ripples and obtain high performance.

Fig. 1 shows the commutation moments detected by the three Hall sensors embedded into the stator [13] and the related current setpoints and back emf for the three phases. The electrical position of the rotor defines which phases are energized [14]. The relation between the electrical and mechanical position can be described as follow:

$$\theta_e = \frac{p}{2}\theta_m \tag{1}$$

Per electrical period, the currents setpoints change at six discrete moments in this way that the two phases that produce the highest torque are energized while the third phase is off.

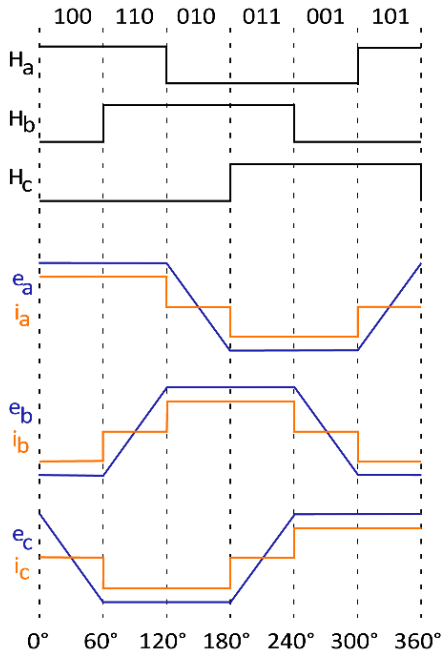

Fig. 1. Ideal back EMF, phase currents and Hall sensor signals per electrical period

Driving a BLDC in its simplest form only needs a six-step inverter drive and discrete position information of the Hall sensors or sensorless position estimation algorithms. The six-step inverter bridge injects the three-phase desired currents in the BLDC motor (Fig. 2). In simulation and practice, a three phase voltage source inverter consisting of six switches is used to convert a DC voltage to three desired phase square currents [15].

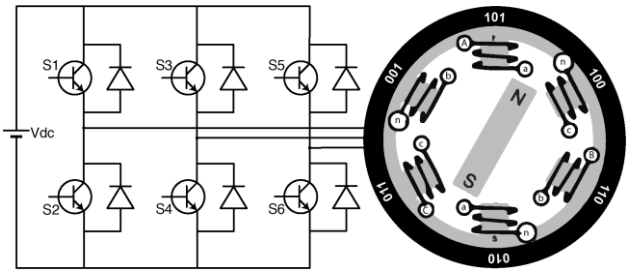

Fig. 2. Six-step inverter bridge and BLDC motor

III. Commutation Based on Hall Sensors

Incorrect placement of the Hall sensors leads to wrong estimation of the commutation moments which causes torque ripples and lower performance. Fig.4 shows the ideal current for a single phase built up from the Hall sensor signals (Fig. 3) and the real and estimated fundamental back EMF. From figure 4 it is clear that the position of the back EMF is estimated correct because the real and estimated back EMF are perfectly aligned. This results in a generated motor torque with low torque ripple (Fig. 5).

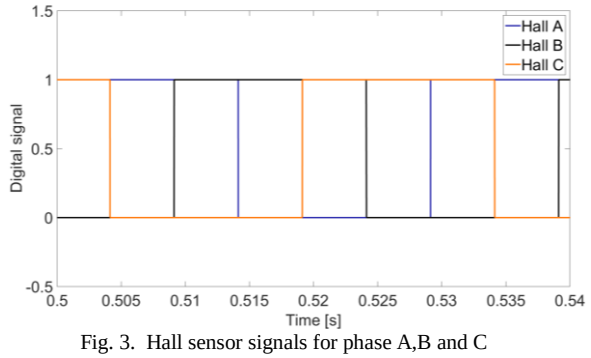

Fig. 3. Hall sensor signals for phase A,B and C

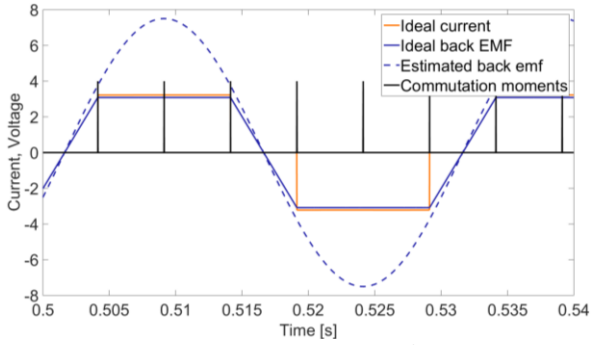

Fig. 4. Ideal current, real and estimated back emf and commutations moments derived from the Hall sensors

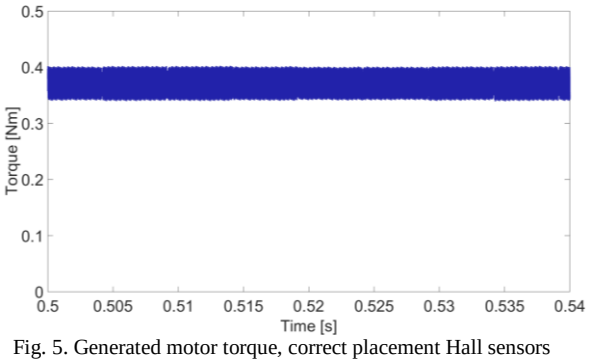

Fig. 5. Generated motor torque, correct placement Hall sensors

If the Hall sensors are shifted by a certain angle, the sensors detects the commutation moments too early or too late. When the current is already non-zero but the back emf is still changing, the commutation goes by too early. Fig. 6 shows the unaligned current and back EMF when the Hall sensors are misaligned 5 electrical degrees. The consequence of this misplacement is that the motor torque is much less constant. The torque peaks are caused by the wrong moments of commutation (Fig. 7).

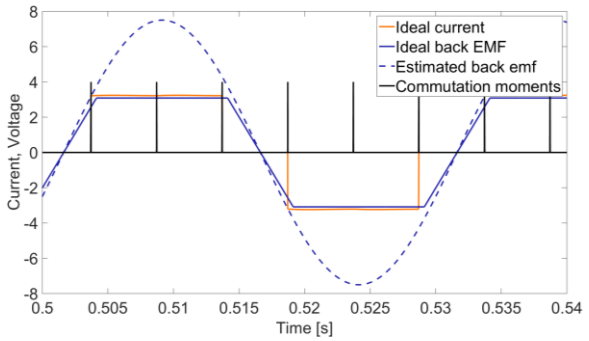

Fig. 6. Ideal current, real and estimated back and commutations moments derived from 5 electrical degrees shifted Hall sensors

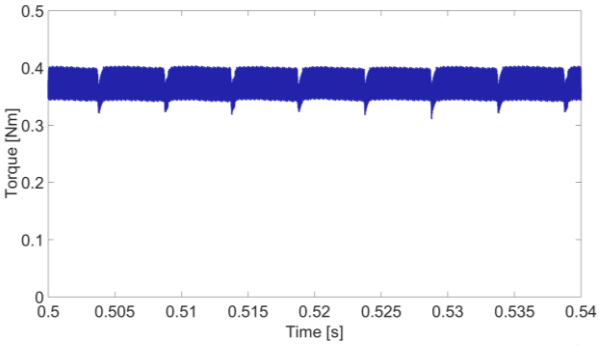

Fig. 7. Generated motor torque, incorrect placement Hall sensors of 5 degrees

IV. Load Angle

In this paper, a self-sensing technique to assess the misalignment is introduced. By estimating the load angle, imperfect placement of the Hall sensors can be easily be detected and accurately quantified.

Maximum torque is generated when the current and back EMF are in phase. In this case, the load angle δ, the

angle between the current vector $\boldsymbol{i}$ and the flux vector $\boldsymbol{\Psi_r}$ is 90° (Fig. 8).

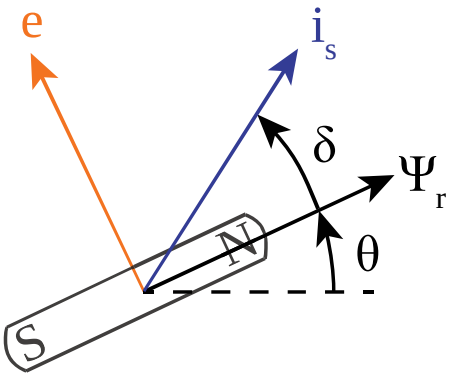

Fig. 8. Vector diagram and load angle

Based on Lenz's law the back EMF vector **e** induced by the rotor flux $\boldsymbol{\Psi_r}$ can be written as:

$$\boldsymbol{e} = C\frac{\mathrm{d}\boldsymbol{\Psi_r}}{dt} \tag{2}$$

Unless an encoder is used, the location of the flux vector is not known. By the lead of 90° of the back EMF vector with respect to rotor flux vector, the load angle can be redefined as:

$$\delta = \frac{\pi}{2} - \angle\boldsymbol{e} - \angle\boldsymbol{i} \tag{3}$$

V. Load Angle Estimation

In the previous equation, the location of the current and the back EMF vectors $\angle\boldsymbol{i}$ and $\angle\boldsymbol{e}$ are unknown. Because the current can be measured directly, the problem of estimating the load angle can be reduced to a problem of estimating the position of the back EMF. The back EMF can be estimated based on the electrical dynamics of the stator windings [16]. If the mutual inductance is neglected [17] [17], the back EMF can be written as:

$$e_a(t) = u_a(t) - R_a i_a(t) - L_a\frac{di_a(t)}{dt} \tag{4}$$

The derivative of the current in eq. (4) will cause problems with noise when implemented. Therefore eq. (3) is transformed to the s-domain:

$$E_a(s) = U_a(s) - R_a I_a(s) - L_a s I_a(s) \tag{5}$$

For sine waves with a pulsation ω, (4) can be written in the frequency domain:

$$E_a(j\omega) = U_a(j\omega) - R_a I_a(j\omega) - L_a s I_a(j\omega) \tag{6}$$

According to [18], the higher harmonics have a negligible contribution to the average torque and can therefore be neglected. For sine wave signals with a fundamental pulsation of ω_1, the equation can be rewritten as:

$$E_a(j\omega_1) = U_a(j\omega_1) - R_a I_a(j\omega_1) - L_a s I_a(j\omega_1) \tag{7}$$

Fourier analysis of the current and voltage measurements are used to determine the fundamental current and voltage components. At discrete time instance k the h^{th} harmonic component $X_h(k)$ based on a period of N samples can be written as:

$$X_h = \sum_{l=0}^{N-1} x\,(k-(N-1)+l)\; e^{jh(\frac{2\pi}{N})l} \tag{8}$$

At each new time instance, the whole sum of the measurements samples have to be reconsidered which is very time consuming. To implement the estimator in a computationally efficient manner, the formula to calculate the Fourier component $X_h(k)$ at time instance k is rewritten as:

$$X_h = \left[X_h(k-1) + x(k) - x(k-N)\right] e^{jh(\frac{2\pi}{N})} \tag{9}$$

One period of samples is needed to calculate the fundamental components. At every time instance, the new DFT is calculated by phase shifting the old DFT, adding the new sample and removing the oldest sample. To tackle this inefficient way of calculating the Fourier components (6), the Sliding Discrete Fourier Transform (SDFT) is used [8], [19]. Fig 9 shows the structure of how the SDFT is implemented in the simulation model.

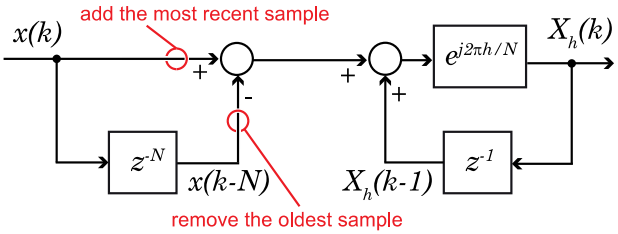

Fig. 9. Implementation of the SDFT

By solving the SDFT at the fundamental frequency, which is equal to the imposed speed, the vector representations of the fundamental components of u_a and i_a can be estimated. The estimation of the back emf e_a is based on the fundamental components of current and voltage measurements and according to this method, the algorithm only needs the electrical parameters such as inductance and resistance for estimating the complex value of the back emf [7], [8] (eq. 7). The estimation of the back emf is leading to an estimation of the load angle (eq. 3). The mechanical load parameters such as inertia or damping have not to be known and changing of this variables have no influence on the estimation. Because the estimation is based on the fundamental components, the presence of higher harmonic components and noise in the measurements have no effect on the quality of the estimation.

VI. SIMULATION RESULTS

In the next part of the paper simulation results are presented. The Simulation model includes the six-step inverter bridge, the BLDC motor, a constant load of 0.1 Nm and the load angle estimator [20]. The data of the modeled BLDC motor are based on the datasheet of Transmotec B8686-24 BLDC motor (nominal voltage 24 V, nominal current 13.76 A, nominal speed 3062 rpm, nominal torque 0.703 Nm, 8 poles).

BLDC motors are ideally suited for high speed applications and are easily controlled in speed. Because position information is available from the Hall sensors, the speed is estimated based on the Hall signals. This feedback of the Hall sensors is used to determine the commutation moments and to control the motor speed (Fig. 10) [21]. Using a high resolution encoder instead of Hall sensors would only increase the prize and the complexity of the application. Only for positioning task an encoder is essential, but then the preference is mostly made for low-cost stepping motors or high-end PMSM [22].

It is clear from Fig. 11 that the resolution of the speed estimation is much bigger than the resolution of an encoder but it is more than adequate to have knowledge about the speed, certainly in the high/constant speed range. After start up, the estimated speed is sufficiently precise to regulate the speed at 500 rpm.

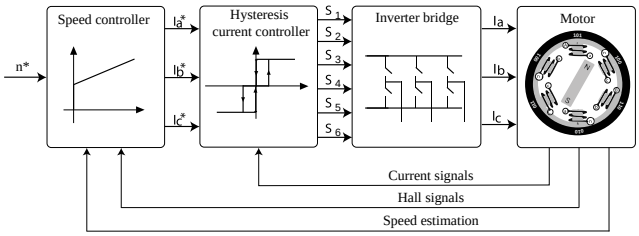

Fig. 10. Control in speed of BLDC motor

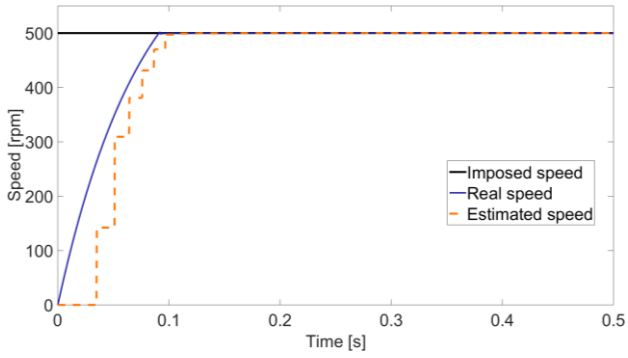

Fig. 11. Speed controlled at 500 rpm

To avoid leakage when applying the SDFT, the window length has to be constant and more or less be equal to the signal period of the electrical signals to achieve correct results. In constant speed operation, the numbers of samples in one period is constant and the window length can also be kept constant. When a new speed setpoint is applied, the window size has to be adapted. During the first period after the change in speed, the SDFT will not deliver good estimation results. A whole new period of samples is necessary to become good estimation results of the fundamental components.

A. *Influence of the misplacing of the Hall sensors on the load angle*

To detect only the influence of the misplacement of the Hall sensors, other effects like the current dynamics have to be excluded. This is done by estimating the load angle based on the ideal current and not on the real current.

Figure 12 shows the estimated load angle for four different shifted Hall sensors at a speed of 500 rpm. The Hall sensors are shifted with 0°,1°,-1° and 5° electrical degree(s) and this is direct visible in the estimated load angle. It can be derived from these results that this small misalignments of the Hall sensors can be accurately detected. Derived from eq. 1, these misalignments are equivalent with a wrong positioning of the Hall sensors of 0°, 0.25°, -0.25°, 1.25° mechanical degree(s). As depicted in blue in Fig. 12, the estimated load angle is 90° and equal to the ideal angle if the Hall sensors are correctly placed. If the Hall sensors are shifted by a certain angle, the sensors detects the commutation moments too early or too late. This results respectively in a load angle bigger or smaller than 90°.

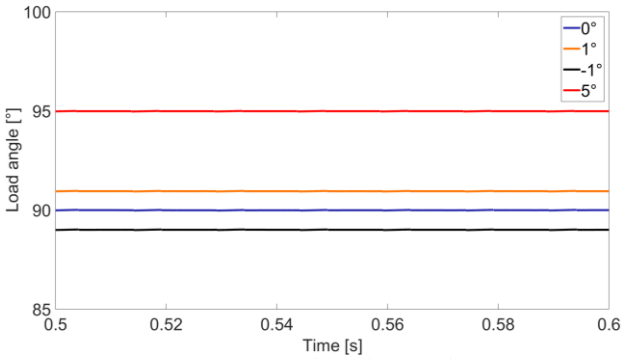

Fig. 12. Load angle estimation for different shifted Hall sensors

B. *Influence of the stator dynamics on the load angle*

In the previous simulation the load angle is estimated based on the ideal current and the estimated back EMF to exclude all the side-effects. In this section the Hall sensors will not be shifted because the influence of the stator dynamics on the load angle will be determined. Due to the dynamics of the stator windings and the response time of the current regulator, the real current is not equal to the ideal current. The dynamics of the stator windings determines the injection of the current and this have also influence on the load angle.

Figure 13 shows the ideal and real current and their fundamental components at a rotating speed of 1250 rpm. The real current lags behind the ideal current.

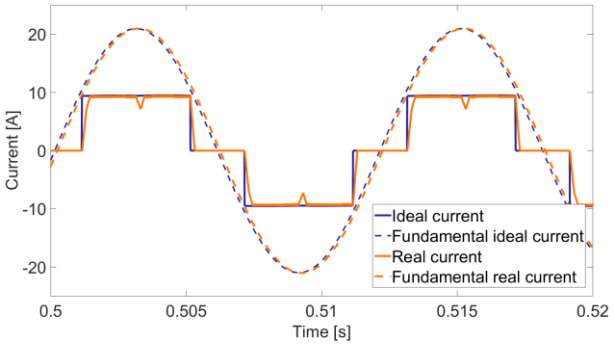

Fig. 13. Ideal and real current and their fundamental components, speed 1250 rpm

As illustrated in Fig. 14 the back EMF is in phase with the ideal current but not with the real current which will result in torque ripples even if the Hall sensors are aligned correctly. The stator dynamics have influence on the difference in phase between the ideal and real current and thus also on the load angle (Fig. 17 load angle for 1250 rpm depicted in brown).

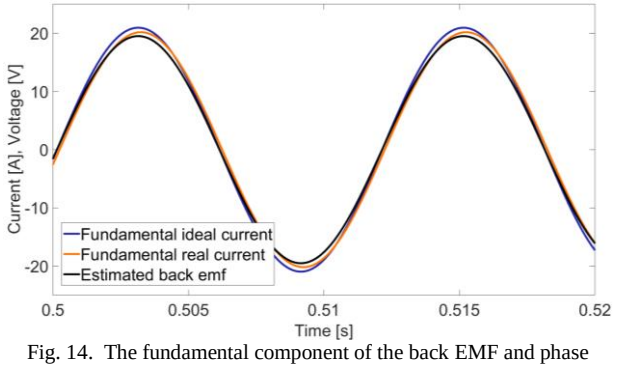

Fig. 14. The fundamental component of the back EMF and phase current, speed 1250 rpm

Fig. 15 and 16 show the ideal and real current for different speed levels of 500 and 1250 rpm. The higher the imposed speed, the higher the motor torque and the higher the asked current level is. The rising/falling time of the current to reach the desired level is thus bigger for higher speeds. The signal period is also smaller for higher speeds, so the contribution of rising and falling of the current with respect to the signal period is higher. This results in an increased phase lag of the real current and a load angle which differs more from the ideal load angle of 90° for higher speeds (Fig. 17).

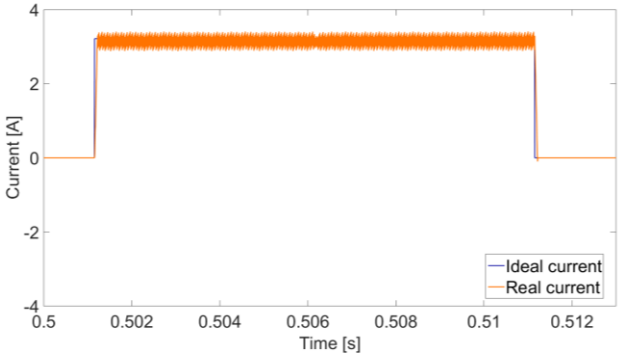

Fig. 15. Ideal and real current at a speed of 500 rpm

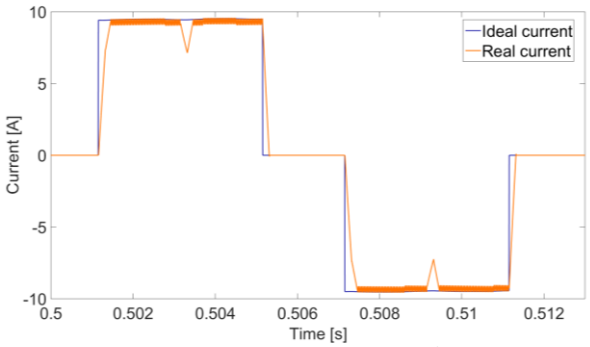

Fig. 16. Ideal and real current at a speed of 1250 rpm

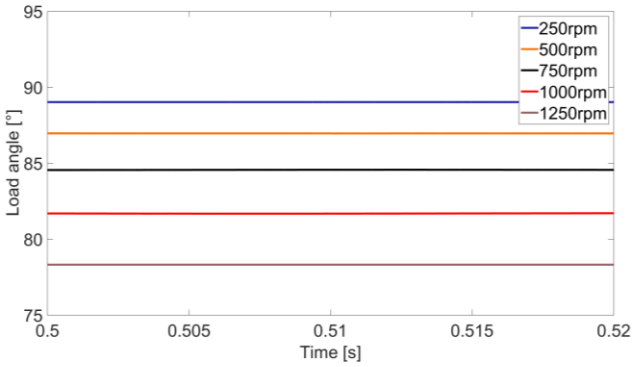

Fig. 17. Load angle estimation for different speeds

VII. Measured results

In this sections real measurements are presented to determine the quality of the commutation. The Transmotec B8686-24 BLDC motor is tested. The controlled speed is equal to 500 rpm using the Hall sensors to determine the commutation moments and to control the speed.

Figure 18 shows the ideal and measured current and the estimated fundamental back EMF. The phase current and back EMF are almost in phase.

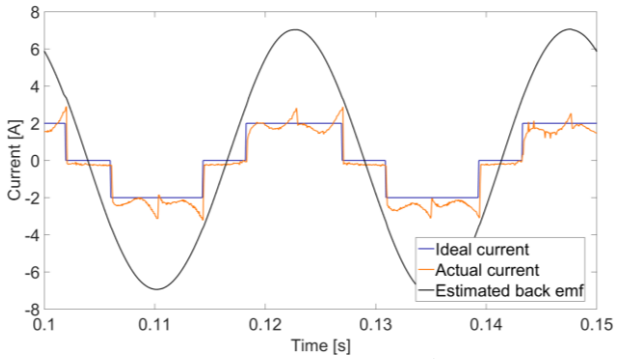

Fig. 18. Ideal and measured current and estimated fundament back EMF

Simulations showed that at 500 rpm the load angle is 87°, which was smaller than ideal angle of 90° (Fig. 17). The small difference of 3° was due to the dynamics of the stator windings because the influence of misplacing of the Hall sensors was excluded. The measured load angle is fluctuating around 88,4° (Fig. 19.). From this result with the simulations, it seems that the placement of the Hall sensors is more or less correct. The Hall sensors give a good approximation of the optimal moments of

commutation, but due to the response of the current controller, the load angle estimation reveal that there is a small difference with the ideal load angle.

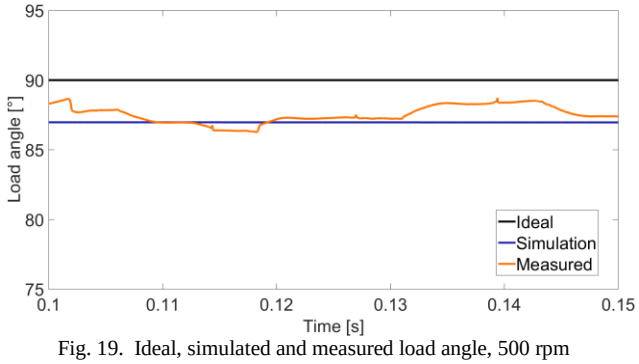

Fig. 19. Ideal, simulated and measured load angle, 500 rpm

VIII. CONCLUSIONS

In this paper, a method is proposed to estimate the load angle of a 3-phase BLDC motor. This self-sensing algorithm needs no tuning and mechanical parameters but is simply based on one voltage and current measurement and the electrical properties of the stator phases.

Simulation and measurement results validate the effect of Hall sensor misplacement and current dynamics on the estimated load angle. To know the influence of this effects separately on the load angle, the load angle is estimated based on the ideal or the real current and the estimated back emf. To detect the misplacement of the Hall sensors, the effect of the current dynamics are excluded by estimating the load angle based on the ideal current and estimated back emf. For optimal torque generation, the load angle must be 90°. This load angle can be used as an indication for the quality of the commutation and torque generation.

Further research will be done to detect the misalignment of the three Hall sensors separately. A solution will be proposed to reduce the misalignment of the Hall sensors and to minimize the influence of the dynamics of the stator windings. Countermeasures will be elaborated to improve the commutation in BLDC motors. This algorithm also gives opportunities for optimization of sensorless algorithms with incorrect zero crossing detection of the back.

ACKNOWLEDGEMENT

Research funded by a PhD grant of the Research Foundation Flanders (FWO).

IX. REFERENCES

[1] J. Shao, “An improved microcontroller-based sensorless brushless DC (BLDC) motor drive for automotive applications,” *IEEE Trans. Ind. Appl.*, vol. 42, no. 5, pp. 1216–1221, 2006.

[2] J. Shao, D. Nolan, M. Teissier, and D. Swanson, “A novel microcontroller-based sensorless brushless DC (BLDC) motor drive for automotive fuel pumps,” *IEEE Trans. Ind. Appl.*, vol. 39, no. 6, pp. 1734–1740, 2003.

[3] D. K. Kim, D. S. Shin, S. T. Lee, H. J. Kim, B. I. Kwon, B. T. Kim, and K. W. Lee, “Novel position sensorless starting method of BLDC motor for reciprocating compressor,” *INTELEC, Int. Telecommun. Energy Conf.*, 2009.

[4] P. Yedamale, “Brushless DC (BLDC) Motor Fundamentals,” *Microchip Technol. Inc.*, pp. 2–5, 2003.

[5] S. Derammelaere, B. Vervisch, F. De Belie, B. Vanwalleghem, J. Cottyn, P. Cox, G. Van Den Abeele, K. Stockman, and L. Vandevelde, “The efficiency of hybrid stepping motors: Analyzing the impact of control algorithms,” *IEEE Ind. Appl. Mag.*, vol. 20, no. 4, pp. 50–60, 2014.

[6] S. Lee and D. Ph, “A comparison study of the commutation methods for the three-phase permanent magnet brushless dc motor,” *Pennsylvania State Univ. Berks Campus*, pp. 3–5.

[7] S. Derammelaere and K. Stockman, “European Patent Application: Control method and device therefor,” 2013.

[8] S. Derammelaere, C. Debruyne, F. De Belie, K. Stockman, and L. Vandevelde, “Load angle estimation for two-phase hybrid stepping motors,” *IET Electr. Power Appl.*, vol. 8, no. 7, pp. 257–266, 2014.

[9] E. Klintberg, “Comparison of Control Approaches for Permanent Magnet Motors,” *Master Sci. Thesis, Chalmers Univ. Technol.*, no. Sweden, pp. 3–5, 2013.

[10] J. Zhao and Y. Yangwei, “Brushless DC Motor Fundamentals Application Note,” *MPS, Futur. Analog IC Technol.*, pp. 7–8, 2011.

[11] P. Kshirsagar and R. Krishnan, “High-efficiency current excitation strategy for variable-speed nonsinusoidal back-EMF PMSM machines,” *IEEE Trans. Ind. Appl.*, vol. 48, no. 6, pp. 1875–1889, 2012.

[12] L. Prokop and L. Chalupa, “3-Phase BLDC Motor Control with Sensorless Back EMF Zero Crossing Detection Using 56F80x,” *Appl. Note*, no. Freescale Semiconductor, pp. 17–18, 2005.

[13] J. C. Gamazo-real, E. Vázquez-sánchez, and J. Gómez-gil, “Position and Speed Control of Brushless DC Motors Using Sensorless Techniques and Application Trends,” *Dep. Signal Theory, Commun. Telemat. Eng. Univ. Valladolid*, pp. 6909–6913, 2010.

[14] P. Voultoury, “Sensorless Speed Controlled Brushless DC Drive using the TMS320C242 DSP Controller,” no. December, 1998.

[15] Zilog, “Three-Phase Hall Sensor BLDC Driver Using The Z16FMC MCU,” *Zilog*, p. 5.

[16] S. Baldursson, “BLDC Motor Modelling and Control – A Matlab ® /Simulink ® Implementation –,” *Master Thesis Work*, pp. 8–13, 2005.

[17] Y. S. Jeon, H. S. Mok, G. H. Choe, D. K. Kim, and J. S. Ryu, “A new simulation model of BLDC motor with real back EMF waveform,” *COMPEL 2000. 7th Work. Comput. Power Electron. Proc. (Cat. No.00TH8535)*, pp. 217–220, 2000.

[18] S. Derammelaere, B. Vervisch, J. Cottyn, B. Vanwalleghem, K. Stockman, S. Derammelaere, F. De Belie, K. Stockman, L. Vandevelde, P. Cox, and G. Van Den Abeele, “ISO efficiency curves of A - Two-phase hybrid stepping motor,” *Conf. Rec. - IAS Annu. Meet. (IEEE Ind. Appl. Soc.*, 2010.

[19] R. Lyons, “dsp tips & tricks - the sliding DFT,” *IEEE Signal Process. Mag.*, vol. 20, no. 2, pp. 74–80, 2003.

[20] F. Verbelen, S. Derammelaere, C. Debruyne, and K. Stockman, “A general model for 6 switch voltage source inverter The generalized model,” *Eur. Conf. Power Electron. Appl.*, pp. 1–7, 2014.

[21] C. W. Hung, C. T. Lin, C. W. Liu, and J. Y. Yen, “A variable-sampling controller for brushless DC motor drives with low-resolution position sensors,” *IEEE Trans. Ind. Electron.*, vol. 54, no. 5, pp. 2846–2852, 2007.

[22] S. Derammelaere, M. Haemers, J. De Viaene, F. Verbelen, and K. Stockman, “A quantitative comparison between BLDC , PMSM , Brushed DC and Stepping Motor Technologies,” *ICEMS*, 2016.